Simulation of topological nodal lines in silicon using Python and Quantum Espresso

Kristoffer Ivik Rosengreen Pedersen
202009792

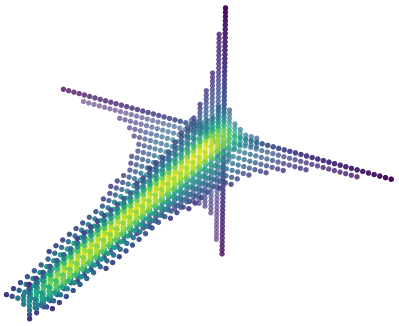

Bachelor's project

Department of Physics and Astronomy
Supervised by Philip Hofmann
Aarhus University

June 2023

Colophon

Simulation of topological nodal lines in silicon using Python and Quantum Espresso

Bachelor's project by Kristoffer Ivik Rosengreen Pedersen.

The project is supervised by Philip Hofmann

Typeset by the author using LaTeX and the memoir document class, using Linux Libertine and Linux Biolinum 12.0/15.36996pt.

The front page figure is of band crossings around the high symmetry point X

The code developed for this bachelor's project is available at `https://github.com/krisrosengreen/bachelorproject`

Printed at Aarhus University

Contents

Chapter 1

Resume

The objective of this bachelor's project is to develop Python software capable of interfacing with the Quantum Espresso software package to dynamically generate control files and band structures across the Brillouin zone of silicon. Specifically, our approach involves the creation of Python software that generates control files interpretable by Quantum Espresso, and subsequently parses and analyzes the software's output. This enables the identification of points or lines of intersection within the band structures.

The primary focus of this bachelor's project lies in the discovery of nodal lines throughout the Brillouin zones, not only restricted to high-symmetry directions or points, but also encompassing off-symmetry directions and points.

Conventional methods for detecting nodal lines typically concentrate on high-symmetry directions, often neglecting comprehensive investigations of the entire Brillouin zone, which includes off-symmetry directions. Consequently, nodal lines not aligned with high-symmetry directions may go undetected. In contrast, our approach utilizes the developed Python software to unveil nodal lines spanning the entire Brillouin zone. Our results exhibit prominent lines along high-symmetry directions that align with those obtained from the tight-binding method, as documented in existing literature [8]. However, our analysis also uncovers unexpected findings, particularly a nodal line along an off-symmetry direction. Further experimental investigation is warranted to ascertain the presence and characteristics of this intriguing line.

Chapter 2

Resume - Danish

Formålet med dette bachelorprojekt er at udvikle Python-software, der kan interagere med Quantum Espreso-softwarepakken og dynamisk generere kontrolfiler og båndstrukturer på tværs af Brillouin-zonen for silicium. Konkret indebærer vores tilgang oprettelsen af Python-software, der genererer kontrolfiler, som Quantum Espresso kan fortolke, og efterfølgende analyserer og behandler softwarens output. Dette gør det muligt at identificere punkter eller linjer med krydsning inden for båndstrukturen.

Det primære fokus for dette bachelorprojekt ligger i opdagelsen af "nodal lines" i hele Brillouin-zonen, ikke kun begrænset til høj-symmetri-retninger eller punkter, men omfatter også asymmetriske retninger og punkter.

Konventionelle metoder til påvisning af "nodal linjer" fokuserer typisk på høj-symmetri-retninger og forsømmer ofte omfattende undersøgelser af hele Brillouin-zonen, inklusive asymmetriske retninger. Som et resultat kan nodale linjer, der ikke er justeret med høj-symmetri-retninger, gå ubemærket hen. I modsætning hertil anvender vores tilgang den udviklede Python-software til at afsløre nodale linjer, der strækker sig over hele Brillouin-zonen. Vores resultater viser fremtrædende linjer langs høj-symmetri-retninger, der stemmer overens med dem, der er opnået ved brug af tight-binding-metoden, som dokumenteret i eksisterende litteratur. Imidlertid afslører vores analyse også uventede fund, især en nodal linje langs en asymmetrisk retning. Yderligere eksperimentel undersøgelse er påkrævet for at fastslå tilstedeværelsen og karakteristika af denne interessante linje.

Chapter 3

Introduction

When atoms combine to form solids, the outermost electrons occupy electronic states that spread throughout the entire solid, known as Bloch waves. Unlike in individual atoms, these states do not have discrete energy levels, but instead depend on the crystal momentum (k) and form bands of energy (E) called $E(k)$ bands. The arrangement of these bands determines various fundamental properties of the solid, including its nature (metal or insulator), conductivity, optical properties, and chemical reactivity. Investigating and calculating band structures is a central objective of solid-state physics.

There are two popular methods for calculating band structures: the tight binding approximation and density functional theory (DFT). This Bachelor's project is inspired by an article by A. Shtyk and C. Chamon [8], where the tight-binding method was employed to study the topological electronic properties of silicon. However, the accuracy of this method can be improved. Hence, the objective of this Bachelor's project is to utilize DFT, a more precise method implemented in a software called Quantum Espresso [6]. Python software is developed to interact with Quantum Espresso, allowing for the dynamic creation of control files and analysis of computational results. The Python software automates the generation of input files for Quantum Espresso and provides a mechanism to read and display the output of the calculations, enabling efficient calculations across the entire Brillouin zone, as opposed to solely along selected high symmetry lines, as done in "traditional" band structure calculations. Conducting such

comprehensive calculations is crucial for identifying band structure features like the topological nodal lines discussed later.

Quantum Espresso is a software specifically designed for DFT calculations, which include band structure calculations. The DFT method employed by Quantum Espresso is more accurate compared to the method used in the article by Shtyk and C. Chamon. Consequently, the aim of this project is to investigate discrepancies and overlaps between these two methods. Conventional calculations often neglect off-symmetry nodal lines or Weyl points, as they do not necessarily align with high symmetry lines in the Brillouin zone. This Bachelor's project seeks to address this limitation by considering such features and incorporating them into the analysis.

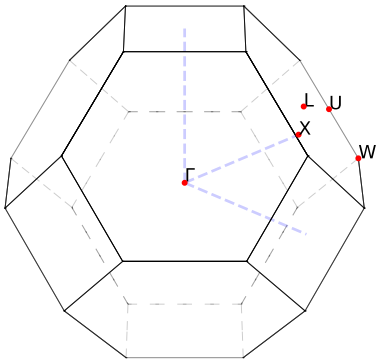

FIGURE 3.1: Illustration of the first fcc Brillouin zone, where high symmetry points are noted.

Chapter 4

Theory

Topological semimetals (TSM) are defined as systems where bands in the valence bands cross each other, this can happen either at discrete points or in closed curves, and this is non-accidental. In other words, perturbations on the Hamiltonian do not remove these points and lines without breaking any of the symmetries. The places where bands overlap in closed curves are often referred to as nodal lines. TSMs in which lines intersect within closed curves in three dimensions are known as topological nodal line semimetals (TNLSM) [3]. One challenge in identifying nodal lines is that they are not always located at high-symmetry points or along a high-symmetry lines. The presence of nodal lines in a material's band structure can have significant implications for its electronic, magnetic, and transport properties. The presence of this can contribute to the appearance of phenomena such as topological insulators or semimetals.

4.1 Tight Binding approximation

The following derivation is taken from this reference [4]. This method constructs a Bloch wave function through a linear combination of atomic orbitals. We start by constructing the Hamiltonian for the atoms that comprise the solid:

$$H_{at} = -\frac{\hbar^2 \nabla^2}{2m_e} + V_{at}(\boldsymbol{r}), \tag{4.1}$$

where V_{at} is the atomic one-electron potential. If there is an atom at every point $\boldsymbol{R}$ of the Bravais lattice, the one-electron Hamiltonian for the solid can be written as

$$H_{sol} = -\frac{\hbar^2\nabla^2}{2m_e} + \sum_{\boldsymbol{R}} V_{at}(\boldsymbol{r}-\boldsymbol{R}) = -\frac{-\hbar^2\nabla^2}{2m_e} + V_{at}(\boldsymbol{r}) + \sum_{\boldsymbol{R}\neq 0} V_{at}(\boldsymbol{r}-\boldsymbol{R}). \tag{4.2}$$

This can be further rewritten.

$$H_{sol} = -\frac{\hbar\nabla^2}{2m_e} + V_{at}(\boldsymbol{r}) + v(\boldsymbol{r}) = H_{at} + v(\boldsymbol{r}), \tag{4.3}$$

where,

$$v(\boldsymbol{r}) = \sum_{\boldsymbol{R}\neq 0} V_{at}(\boldsymbol{r}-\boldsymbol{R}). \tag{4.4}$$

We consider the case where the atoms are far from each other. Here we use the atomic wave function $\phi_n(\boldsymbol{r})$ belonging to the atomic energy levels E_n to calculate the energy eigenvalues of the solid:

$$\int \phi_n^*(\boldsymbol{r}) H_{sol}\phi_n(\boldsymbol{r})d\boldsymbol{r} = E_n + \int \phi_n^*(\boldsymbol{r})v(\boldsymbol{r})\phi_n(\boldsymbol{r})d\boldsymbol{r} = E_n - \beta, \tag{4.5}$$

where β is a small shift in the atomic energy level due to the presence of other atoms. If the atoms are far away from each other, $\beta = 0$. The wave function of the solid is

$$\psi_{\boldsymbol{k}}(\boldsymbol{r}) = \frac{1}{1/\sqrt{N}} \sum_{\boldsymbol{R}} e^{i\boldsymbol{k}\cdot\boldsymbol{R}}\phi_n(\boldsymbol{r}-\boldsymbol{R}). \tag{4.6}$$

We can now calculate the band structure

$$E(\boldsymbol{k}) = \int \psi_{\boldsymbol{k}}^*(\boldsymbol{r}) H_{sol}\psi_{\boldsymbol{k}} d\boldsymbol{r} \tag{4.7}$$

$$= \frac{1}{N}\sum_{\boldsymbol{R},\boldsymbol{R}'} e^{i\boldsymbol{k}\cdot(\boldsymbol{R}-\boldsymbol{R}')} \int \phi_n^*(\boldsymbol{r}-\boldsymbol{R}')H_{sol}\phi_n(\boldsymbol{r}-\boldsymbol{R})d\boldsymbol{r} \tag{4.8}$$

4.2 Density Functional Theory

In describing DFT first step is to introduce the Hohenberg-Kohn energy, $F_{HK}[n(\boldsymbol{r})]$, where $n(r)$ is the electron ground-state density. This is equal to the difference between the ground-state energy and the potential energy [1]. One crucial fact that is needed in the derivation of DFT comes from Hohenberg-Kohn: The ground state density $n(r)$ determines the external potential energy. In other words, for a given density, the potential can be uniquely determined. Another crucial fact is that the total energy of the system is minimal when the density represents the density present in the ground-state [2]. We have the Hohenberg-Kohn free-energy functional[1] given as

$$F_{HK}[n(\boldsymbol{r})] = F_{ni}[n(\boldsymbol{r})] + E_{es}[n(\boldsymbol{r})] + E_{xc}[n(\boldsymbol{r})], \tag{4.9}$$

where $F_{HK}[n]$ is the Hohenberg-Kohn free-energy functional. $F_{ni}[n]$ is the non-interacting kinetic energy. That is, the kinetic energy of a system of noninteracting particles with density $n(\boldsymbol{r})$ $E_{es}[n]$ and $E_{xc}[n]$ are two interaction terms, the electrostatic energy and the exchange-correlation energy. The exchange-correlation energy accounts for the electron-electron interactions in the many body system. The Hohenberg-Kohn free energy describes the total energy of a system in terms of its electron density [1].
We have the Schrödinger equation given as

$$\left(-\frac{\hbar^2}{2m}\nabla^2 + v_{eff}(\boldsymbol{r})\right)\psi_i(\boldsymbol{r}) = \epsilon_i\psi_i(\boldsymbol{r}). \tag{4.10}$$

Given the solutions $\psi_i(\boldsymbol{r})$ this can be used to calculate the total electron density

$$n(\boldsymbol{r}) = \sum_{i=1}^{N} |\psi_i(\boldsymbol{r})|^2. \tag{4.11}$$

The kinetic energy is given by,

1: Theory of functionals and functional derivatives will not be given here, but a brief overview can be found in this reference [1].

$$F_{ni}[n(\boldsymbol{r})] = \sum_{i=1}^{N} \left\langle \psi_i | \hat{t}_i | \psi_i \right\rangle = \sum_{i=1}^{N} \epsilon_i - \int d\boldsymbol{r} n(\boldsymbol{r}) v_{eff}(\boldsymbol{r}). \tag{4.12}$$

The effective potential can be found by taking a functional derivative of the expression for $F_{HK}[n]$.

$$v_{eff}(\boldsymbol{r}) = v(\boldsymbol{r}) - e\varphi(\boldsymbol{r}) + v_{xc}(\boldsymbol{r}), \tag{4.13}$$

where,

$$\varphi = -e \int d\boldsymbol{r}' \frac{n(\boldsymbol{r}')}{|\boldsymbol{r} - \boldsymbol{r}'|}. \tag{4.14}$$

The exchange-correlation potential is defined as

$$v_{xc}(\boldsymbol{r}) = \frac{\delta E_{xc}}{\delta n(\boldsymbol{r})}. \tag{4.15}$$

Thus, you can find $v_{eff}(\boldsymbol{r})$ from $n(\boldsymbol{r})$ for a given $v(\boldsymbol{r})$. These equations are called the Kohn-Sham equations of DFT, and with this mechanism, the band structure can be found. This derivation was taken from this reference [1].

4.3 Symmetries

4.3.1 Spatial Symmetries

The symmetries of nodal lines in spatial coordinates are intimately tied to the characteristics of the underlying potential or wave equation. Reflection symmetry, often encountered in symmetric potentials, manifests as nodal lines that exhibit mirror-like symmetry with respect to reflection planes. Rotational symmetry results in nodal lines that possess rotational symmetry about the axis of rotation. Similarly, systems with translational or inversion symmetries can give rise to nodal lines that exhibit periodic patterns or symmetry with respect to an inversion center, respectively. Understanding these spatial symmetries aids in predicting and interpreting the spatial distribution of nodal lines in various wave phenomena [3].

4.3.2 Spin-Rotation Symmetry

Incorporating the intrinsic property of spin in wave functions introduces spin-rotation symmetry considerations. The behavior of nodal lines with respect to spin-rotation depends on the spin structure and interactions in the system. In some cases, nodal lines may remain invariant under spin rotations, reflecting spin-invariant nodal lines. However, in systems with spin-dependent interactions or strong spin-orbit coupling, nodal lines can exhibit spin-dependent behavior, wherein the arrangement of nodal lines undergoes changes with spin transformations [3].

4.3.3 Symmetry Breaking

Nodal lines are protected by different symmetry groups. When these are broken the nodal lines will break into several nodal points, or it may also be fully gapped. Nodal lines can be broken into point nodes by spin-orbit coupling. This happens because when spin-orbit coupling is considered, band repulsion between opposite spins becomes nonzero at finite momenta, making the nodal line unstable. This nodal line can then be broken down into several pairs of Weyl points, one or several Dirac points, two separate nodal lines or become fully gapped [3].

4.4 Weyl Nodes

Weyl semimetals are three dimensional solids where electronic bands accidentally cross at a single, isolated point in three dimensional $\boldsymbol{k}$-space of the Brillouin zone. An accidental degeneracy point is called a Weyl node [9].

Chapter 5

Method

5.1 Development of software to find nodal lines

This bachelor's project is a simulation of topological nodal lines in Si using Python and Quantum Espresso. The aim of this bachelor's project is to develop software that can systematically search for nodal lines that are not only present in high symmetry directions, but also in off-symmetry directions, which are difficult to find using conventional methods. Nodal lines throughout the Brillouin zone are here found by calculating band structures in a 3D grid within the Brillouin zone. This is accomplished by creating Python software that interfaces with Quantum Espresso using a specific pseudo-potential for Si [5]. An illustration of the method to finding nodal lines throughout a section of the Brillouin zone is shown in figure 5.1. Specifically, in a section of the Brillouin zone, we calculate band structures as a grid of columns that can be combined to find points or lines, where the bands intersect or overlap. Practically, finding points or lines of intersection means that the energy differences between bands at a given $\boldsymbol{k}$-value are within an energy threshold. However, this does not necessarily mean that a nodal line or point has been found even if the threshold criterion is met. Conversely, given that the grid is sampled with points that have discrete distances to each other, means that the sampling may not encompass all nodal lines or points at a reasonable distance to be picked up by the energy differences threshold, even though they exist.

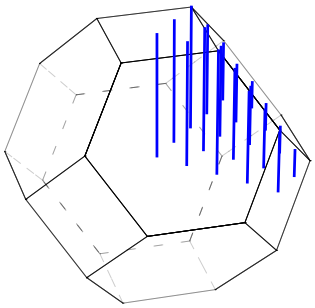

FIGURE 5.1: Illustration of how nodal lines in the Brillouin zone are found. Several columns across a single corner, corresponding to 1/8 of the fcc Brillouin zone, are calculated using the developed Python software that interfaces the Quantum Espresso software package. This gives band structures for the given $\boldsymbol{k}$-points across a given column. However, for the actual calculations, the columns are packed more closely than shown here, such that nodal lines are more likely to be found.

Quantum Espresso is interfaced by control files dynamically created using Python. The control files specify the $\boldsymbol{k}$-points, kinetic energy cut-off and lattice constant, for the band structure calculation. However, before band structure calculations are done, Quantum Espresso must do a self-consistent calculation, which finds the appropriate electron ground-state density used for the band structure calculations. Now, these files control files, in combination, create band structures across the Brillouin zone that allows for detecting nodal lines and nodal points across the Brillouin zone. The development of this software for interfacing Quantum Espresso and calculating 3D nodal lines has amounted to significant proportion of effort for this bachelor's project and close to 2000 lines of code. The code developed for this bachelor's project is available at GitHub[1].

1: The code is available at https://github.com/krisrosengreen/bachelorproject

5.2 Testing the software

Testing the software is crucial. Here, we test that we get a sufficient number of eigenvalues for the band structure calculation. This is simply done by checking that we obtain 8 values for a given $\boldsymbol{k}$-point. We must test that the total energy of the system converges. This is simply done by changing the kinetic-energy cutoff that is controlled by Quantum Espresso - The total energy of the system must converge when we increase the kinetic-energy cutoff. Lastly, we also obtain the lattice constant used in all calculations by finding the lattice constant value that produces an overall smallest attainable total energy of the system. This is simply done using a downhill simplex algorithm [7].

As the software is unable to calculate kinetic energy from zero to infinity, a reasonable kinetic energy cutoff value must be selected such that most of the energy is included in the calculations. The value must be chosen such that it encompasses the total energy of the system and is not so high as to be more computationally expensive than necessary. Here, a value of 30 Ry was chosen, and the reasoning for choosing this value will be shown later.

Chapter 6

Simulation

6.1 Preliminary calculations

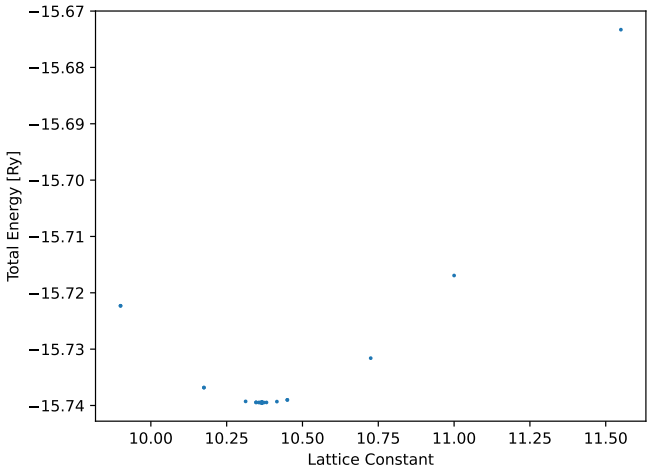

Figure 6.1: Optimization of the lattice constant. The lattice constant corresponding to the lowest attainable system energy must be used for accurate Si calculations.

The first step is to determine the appropriate kinetic-energy cutoff value to be used in all of our calculations. Thereafter, the appropriate lattice constant that minimizes the total energy of the system has

to be determined. From figure 6.2 we can see that the total energy converges sufficiently at kinetic energy cutoff of 30 Ry. Given the fact that a higher energy cutoff also leads to a longer computation time, I set this parameter to 30 Ry for all calculations. From figure 6.1 the optimal lattice constant is obtained to be LC = 10.366. This is the lattice-constant value that will be used for all the following calculations.

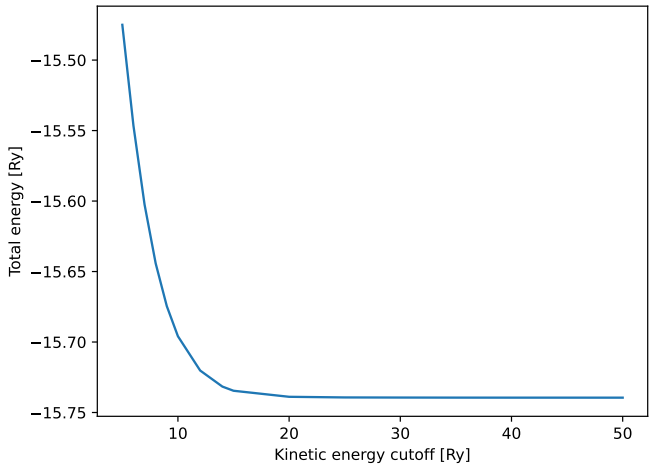

FIGURE 6.2: Total energy of the system is dependent on the kinetic energy cutoff used in the Quantum Espresso calculations.

In the article by A. Shtyk and C. Chamon, the authors use tight binding method to calculate band structures [8], the results they obtain can be seen in figure 6.3. From this figure it can be seen that nodal lines are present along the following high symmetry path, Γ-L-X-W-U. Specifically, the red lines represent nodal lines in both the valence and conduction band. The lines marked in red are not the only nodal lines present in the band structure. Specifically, there are also nodal lines present along the high symmetry directions, Γ-L and Γ-X. These nodal lines are similarly present in the figure we obtained using our DFT calculation with our software. The difference between these results, the results from known literature, and our band structure calculation, is the difference in band dispersion.

In our Python software we can calculate the band structure for Si along the following high-symmetry path, L-Γ-X-W-U-Γ. Figure 6.4

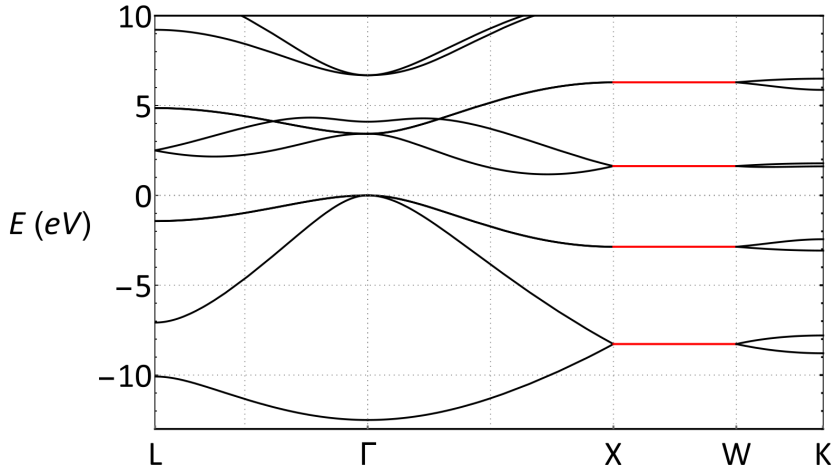

FIGURE 6.3: Nodal lines taken from literature that inspired this bachelor's project [8] .

shows the band structure of Si along the same high-symmetry directions as the tight-binding result in figure 6.3 but using DFT as implemented in Quantum Espresso.

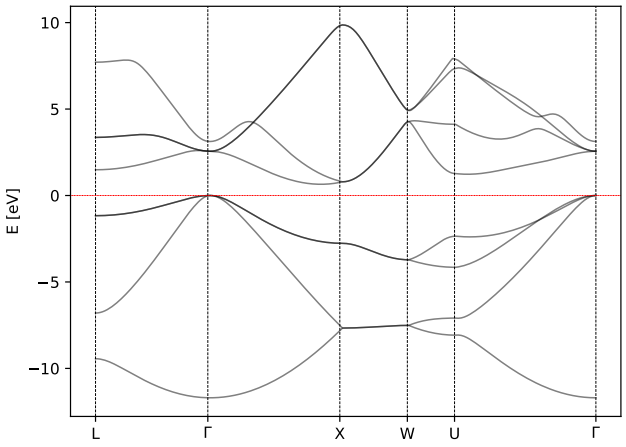

FIGURE 6.4: Band structure calculation along high symmetry points in Si.

6.2 Nodal lines

We know that the band structures in the Brillouin zone are symmetric across the Brillouin zone, because of the symmetry of the solid's Hamiltonian. Therefore, it is sufficient to only look at an irreducible section of the Brillouin zone. Consequently, we can achieve more detailed structures across the Brillouin zone for less spent computation time, thereby facilitating the process of uncovering nodal lines.

We now do high-resolution, three-dimensional calculation around all high-symmetry points, to get a more precise look of nodal lines around these high-symmetry points. That is, we create a tightly-bound network of columns that, in combination, can find points where bands, irrespective of energy, intersect. These columns have to be as tightly packed as computationally reasonable. Here we look at a mesh of 150 by 150 columns, where each column consists of 150 points. As can be seen in the figures 6.5-6.8, we are only looking at a single section of the Brillouin zone. The reason for this is that it is, again, because it is computationally expensive to find nodal lines in the entire Brillouin zone. To circumvent this we exploit the symmetry of the solid's Hamiltonian such that we only need to do calculations within an irreducible part of the Brillouin zone. This section corresponds to the volume that encloses the points present in figure 6.9. In figures 6.5-6.8 we see all the nodal lines we expect from figure 6.9. We do not see any nodal lines around U, as expected in figure 6.9. This is so even when high-resolution calculations are done around this symmetry point. The nodal lines present in figure 6.8 are more prominent, due to a slower band dispersion around this point. Therefore, more points fulfill the threshold criterion.

We now do a calculation across a section, corresponding to 1/8 of the Brillouin zone, to find nodal lines. This we do by creating a mesh of grids as illustrated in figure 5.1. In figure 6.9 we see dots throughout the 3D-plot. These dots represent locations, in three-dimensional momentum-space, where bands intersect at any given energy in the valence band. These points in combination reveal nodal lines present in the Brillouin zone of Si, and the interesting part of this is that these nodal lines revealed with our method do not have to follow high-symmetry paths as conventional methods do. The nodal lines seen in figure 6.4 can be seen in figure 6.9. To put it clearly, the

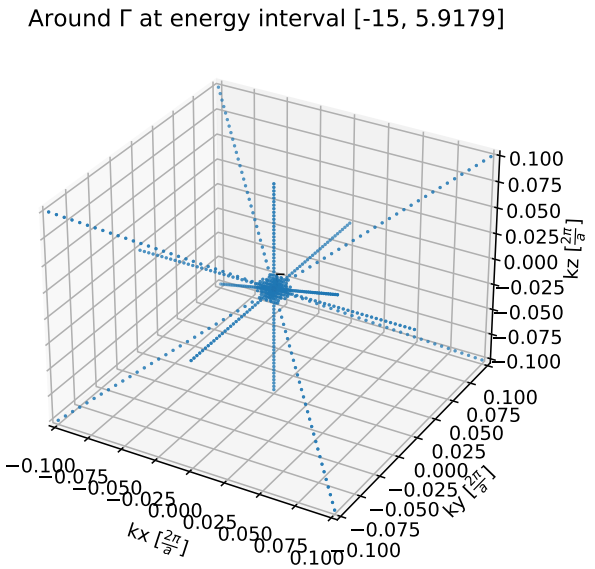

FIGURE 6.5: Nodal lines around Γ symmetry point.

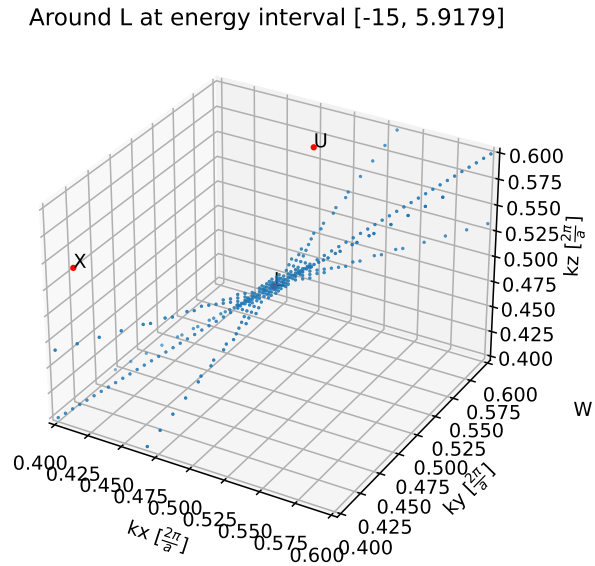

FIGURE 6.6: Nodal lines around L symmetry point.

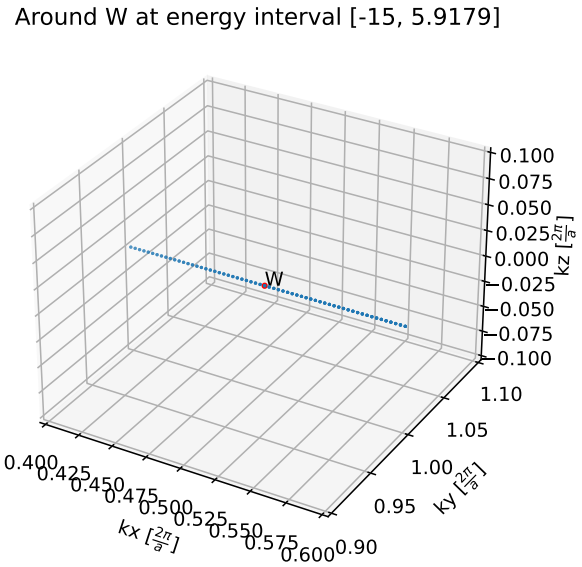

FIGURE 6.7: Nodal lines around W symmetry point.

nodal line present between the points X and L are present, because of the blue line that connects these points in figure 6.9. And, this blue line is present because the software recognized the existence of a nodal line from the energies of bands being so close (Difference being smaller than the given threshold) as to roughly be equal. Moreover, the blue line between Γ and X also represent a nodal line between these two points. The blue line that connects Γ and L also represents a nodal line between these two points. Lastly, the remaining blue lines are result of the symmetry of the solid's Hamiltonian. For example, the line seen between Γ and $(1, 0, 0)\frac{2\pi}{a}$ is entirely the same as the line between Γ and X, but reflected.

There is an unexpected nodal line in figure 6.9 represented by the red line, which goes from L to around $(0.4, 0, 0)\frac{2\pi}{a}$. Although the line in question is not entirely linear, it curves slightly. If we calculate the band structures between the two points we get the results shown in figure 6.10. The two uppermost valence bands appear to overlap. However, this is not entirely certain, because the nodal line, as seen in figure 6.9, is not entirely straight, whereas this calculation assumes

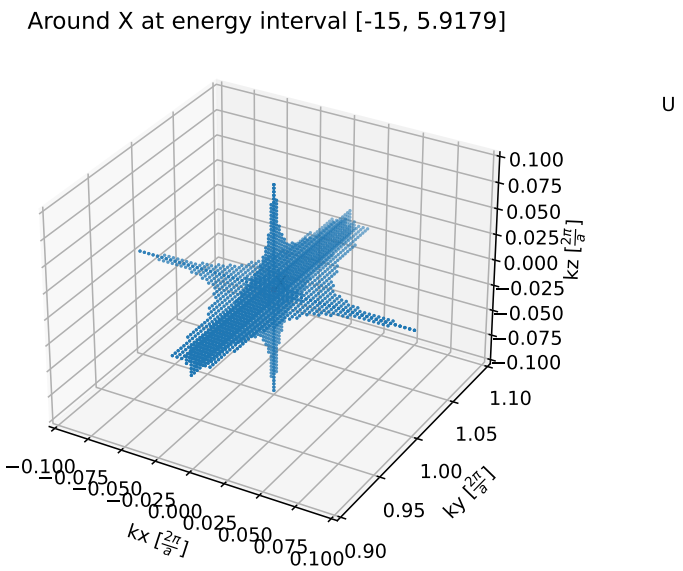

FIGURE 6.8: Nodal lines around X symmetry point. The nodal lines are more prominent in this figure than others.

it is. This line is entirely unexpected as it does not lie on a high-symmetry path, and is only revealed in our results, as opposed to conventional methods, because we have looked at the entire Brillouin zone encompassing both high-symmetry and off-symmetry directions in our calculations. Lastly, this line would be interesting to investigate experimentally to see if the nodal line exists.

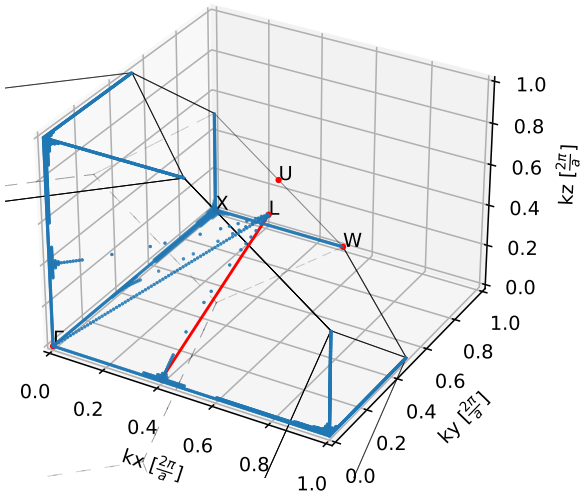

FIGURE 6.9: Figure of nodal lines along all valence energies across the Brillouin zone. High symmetry points have been marked as well. The solid lines represent borders of the fcc-lattice. The red line represents the approximate path of the unexpected line. It is approximate because the line is not straight, but curved - The band structure of this same line can be seen in figure 6.10.

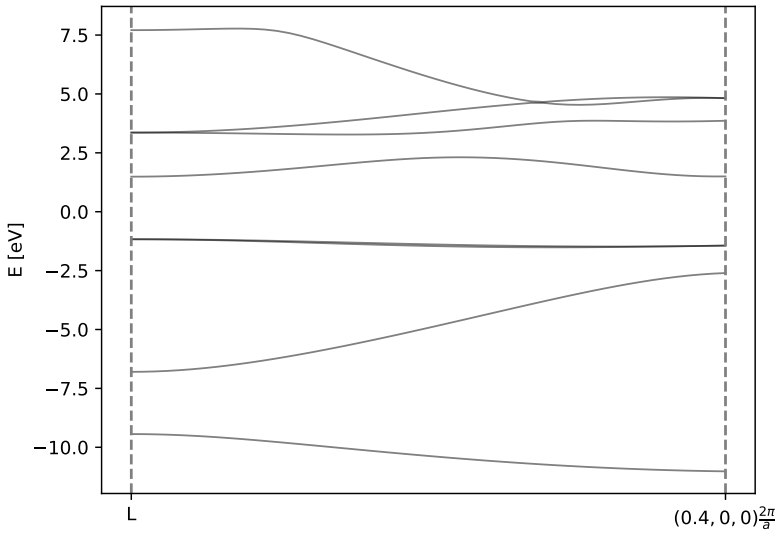

FIGURE 6.10: A nodal line between the points L and $(0.4, 0, 0)\frac{2\pi}{a}$. The two uppermost bands in the valence structure do not entirely overlap. This is because the nodal line is not entirely linear.

Chapter 7

Conclusion

There exists two popular methods of calculating band structure: Tight binding approximation and density functional theory. This bachelor's project was inspired by nodal lines calculated using tight binding approximation, and was inspired to use the more accurate theory, density functional theory, to see if there are nodal lines we can find which were not present from tight-binding approximation. Specifically, Python software was developed to interface Quantum Espresso, by dynamically creating control files, and analayzing and parsing the output of the software. The developed software can find nodal lines that are not only on symmetry points or along symmetry lines, but also at off-symmetry points throughout the Brillouin zone. From this we found the same nodal lines as in the tight binding approach as we did using our approach. However, we also seem to have found a line of interest in the Brillouin zone that is not along high symmetry directions, which would be interesting for future experimental study to ascertain its existence. This could be found because of the tool we developed to look for nodal lines across the Brillouin zone, in not only high-symmetry directions, but also off-symmetry directions.

Bibliography

[1] Nathan Argaman and Guy Makova. 'Density Functional Theory - an introduction'. In: *Proc. London Math. Soc.* (1999).

[2] Eberhard Engel and Reiner M Dreizler. *Density functional theory*. en. 2011th ed. Theoretical and mathematical physics. Berlin, Germany: Springer, Feb. 2011.

[3] Chen Fang et al. 'Topological nodal line semimetals'. In: *Chinese Physics B* (Sept. 2016).

[4] Philip Hofmann. *Solid state physics*. en. 2nd ed. Weinheim, Germany: Wiley-VCH Verlag, Apr. 2015.

[5] *Pseudo-potential used in Quantum Espresso calculations*. URL: http://pseudopotentials.quantum-espresso.org/upf_files/Si.pbe-rrkj.UPF.

[6] Quantum ESPRESSO Foundation. *Quantum ESPRESSO*. Version 7.2. URL: https://www.quantum-espresso.org/.

[7] *scipy.optimize.fmin*. URL: https://docs.scipy.org/doc/scipy/reference/generated/scipy.optimize.fmin.html.

[8] A. Shtyk and C. Chamon. 'Topological electronic properties of silicon'. In: *Physical review* (2020).

[9] Grigory Tkachov. *Topological Quantum Materials*. 1st edition. Jenny Stanford Publishing, Aug. 2022.